SYMPOSIUM on FLOW-INDUCED VIBRATIONS

VOLUME 5
TURBULENCE-INDUCED NOISE AND VIBRATION OF RIGID AND COMPLIANT SURFACES

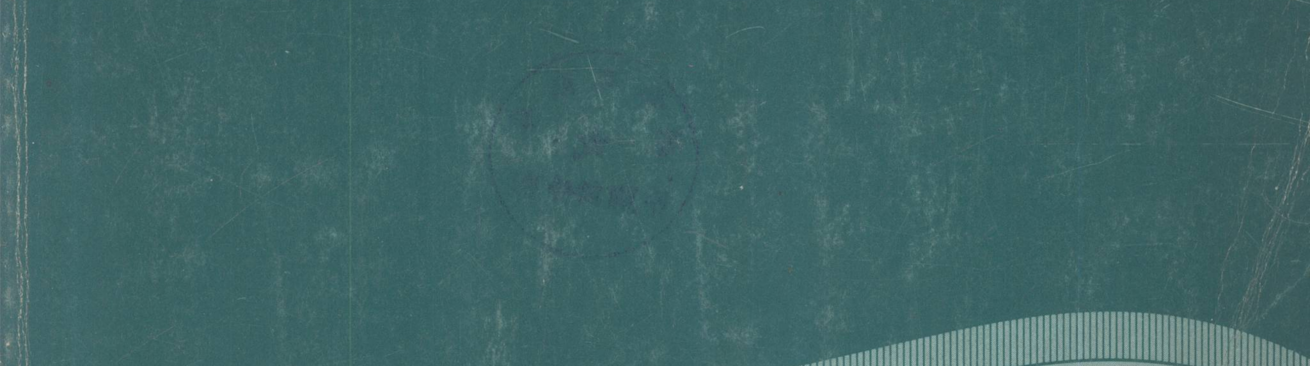

Editors
M.P. PAIDOUSSIS
A.J. KALINOWSKI

SYMPOSIUM on FLOW-INDUCED VIBRATIONS

VOLUME 5
TURBULENCE-INDUCED NOISE AND VIBRATION OF RIGID AND COMPLIANT SURFACES

Presented at

THE ASME WINTER ANNUAL MEETING
NEW ORLEANS, LOUISIANA

DECEMBER 9 -14, 1984

Symposium co-sponsored by

Applied Mechanics, Fluids Engineering, Heat Transfer, Noise Control and Acoustics, Nuclear Engineering, and Pressure Vessels and Piping Divisions

Sessions in this Volume co-sponsored by

APPLIED MECHANICS AND NOISE CONTROL AND ACOUSTICS DIVISIONS

Edited by

M.P. PAIDOUSSIS (Principal Editor)
McGill University
Montreal, Quebec, Canada

A.J. KALINOWSKI
Naval Underwater Systems Center
New London, Connecticut

THE AMERICAN SOCIETY OF MECHANICAL ENGINEERS
United Engineering Center 345 East 47th Street New York, N.Y. 10017

Library of Congress Catalog Card Number 84-72467

8660603

PREFACE

The 1984 ASME Symposium on Flow-Induced Vibration is a unique event in the annals of technical meetings organized by ASME. Apart from promising to be one of the most important symposia anywhere on this topic in recent memory (only time will tell exactly how important), it is the first time that such a large symposium on the subject has been organized by ASME. Furthermore, it is the first time that no less than six Divisions of the ASME have cooperated in co-sponsoring a symposium on any given subject, which surely bespeaks of the importance of the subject matter of this particular Symposium. The participating Divisions are:

Applied Mechanics, Fluids Engineering, Heat Transfer, Noise Control and Acoustics, Nuclear Engineering, and Pressure Vessels and Piping.

I should like to thank them all, for without their support this Symposium would not have been the success that it is promising to be.

The Proceedings of the Symposium are published in six bound volumes, containing sixty-eight papers in all, as follows:

Volume 1 Excitation and Vibration of Bluff Bodies in Cross Flow
Volume 2 Vibration of Arrays of Cylinders in Cross Flow
Volume 3 Vibration in Heat Exchangers
Volume 4 Vibration Induced by Axial and Annular Flows
Volume 5 Turbulence-Induced Noise and Vibration of Rigid and Compliant Surfaces
Volume 6 Computational Aspects of Flow-Induced Vibration

The organization of a Symposium of this size, with world-wide participation (from 12 countries), has been both a challenging and rewarding experience. It entailed a great deal of work by many people: the session developers, the reviewers, ASME Headquarters' staff, the 1984 WAM Organizers and, of course, the authors. Of the many people involved, too numerous to mention by name here, I am specially indebted to the session developers and co-editors (O. M. Griffin, M. Sevik, M. K. Au-Yang, S. -S. Chen, J. M. Chenoweth, M. D. Bernstein and A. J. Kalinowski), and would like to single out two: Dr. M. K. Au-Yang and Dr. S. -S. Chen, whom I would like to thank for their unswerving support from the very beginning, when the possibility of a "multidivisional symposium" looked like a pie in the sky! I would also like to thank my secretary, Ruth Gray, for efficiently handling the enormous amount of paperwork involved in several passes of sixty-eight-plus papers across my desk.

Michael P. Paidoussis
Principal Symposium Coordinator
and Principal Editor

FOREWORD

The study of the growth of a boundary layer on flat and curved rigid surfaces has been the traditional realm of classical viscous aerodynamics and hydrodynamics, which began with the "discovery" of the existence of the boundary layer by L. Prandtl at the beginning of the century, and has grown exponentially ever since. Then followed the study of the pressure field generated in the boundary layer, with special interest to the vibration of the surfaces (in the case of flexible or flexibly mounted surfaces), as well as in the sound radiated from these surfaces.

However, in recent years, it has become well established that the development of a boundary layer on a truly compliant surface is not necessarily similar to that on a rigid or sensibly rigid surface. The pioneering experiments of Kramer and the theoretical work of T. Brooke Benjamin and M. T. Landahl in the early 1960's should be mentioned here; also, the more recent analytical work of F. E. Ffowcs-Williams and A. P. Dowling for applying the Lighthill sound analogy towards turbulent-boundary-layer noise predictions. Indeed, it has been found that transition to turbulence may be significantly retarded by surface compliance, to which, among other things, has been attributed the efficient swimming of dolphins, as well as opening the possibility of more efficient propulsion of submarines and surface craft. Of course, the resulting wall-pressure field is also different, as is the radiated sound field. Thus was created the relatively new field of research on turbulence-induced noise and vibration of compliant surfaces.

The seven papers in this volume, Vol. 5 of the Symposium Proceedings, make a significant contribution in the field, with both theoretical and experimental studies on the flow-induced excitation and vibration of compliant surfaces. The first two papers are concerned with the measurement of motions of the compliant surface induced by pressure fluctuations in the turbulent boundary layer (TBL), while the following two papers switch the emphasis to the fluid side of the TBL-structure interaction and focus on measurements of the wall-pressure spectrum, with special attention to the low-wave number noise components. In the last group of papers, theoretical aspects of turbulence are treated, where the TBL pressure at the fluid/compliant-surface interface is first computed by a simulation scheme and, in the last papers, by employing Dowling's extention of the Lighthill sound analogy.

We would like to thank the authors for their cooperation in submitting papers of high quality to this Symposium, and specifically on the topic of this volume of the Proceedings, as well as for their willingness to participate and share their experience with others in this Symposium. We would also like to thank the reviewers for their thoughtful comments and for the experience they have brought to bear in the review process, which has ensured the selection of only worthy papers for the Symposium and contributed to the improvement of those finally accepted.

M. P. Paidoussis

A. J. Kalinowski

CONTENTS

A NONCONTACTING ELECTROOPTIC DISPLACEMENT SENSOR FOR PIEZOELECTRICALLY DRIVEN ACTIVE SURFACES*

S. A. Cerwin
Southwest Research Institute
San Antonio, Texas

ABSTRACT

A noncontacting electrooptic displacement sensor for the measurement of the motion of a piezoelectrically excited active wall is described. The active wall was constructed and studied as part of a program conducted for the Office of Naval Research to investigate the drag reduction properties of an actively driven surface in turbulent water flow. The sensor employed a two arm optical triangulation method with a two element position sensitive detector to monitor the surface displacements from a stand-off distance of 23 cm (9 inches). Designed to operate in either an air or water medium, the displacement sensor demonstrated better than 1.3 μm (50 μ-inch) resolution over displacement ranges of approximately 1.3 mm (.05-inch). The system was implemented in two different configurations: one using an infrared LED light source and the other a visible red helium-neon laser source. In both cases, the light source was modulated, and a phase locked detector was used to reject unwanted ambient light. Spot size was an adjustable parameter and was set to 1 mm (.04-inch) for this application. The displacement monitor was articulated in three axes on precision translation stages to cover a 5 cm x 13 cm (2-in. x 5-in.) area. The system was successfully used to monitor accurately displacements on the order of 25 μm (.001-inch) peak-to-peak on an active wall driven by piezoelectric transducers over an acoustic frequency range from DC to 150 Hz.

INTRODUCTION

This paper describes a noncontacting electrooptical displacement sensor developed to monitor the motions of a piezoelectrically excited active wall with peak-to-peak displacements on the order of 25 μm. The active wall was devised in a program conducted for the Office of Naval Research† to investigate the drag reduction properties of an actively driven surface in turbulent water flow. The active portion of the wall was constructed by stretching a thin, diffusely reflecting mylar membrane over an array of piezoelectric pushers spaced at an interval of 1.25 mm. A cross sectional view of the wall construction is given in Figure 1. Because each of the peizoelectric elements could be driven independently, proper adjustment of the phase and amplitude of individual drive wave-

*Supported by the Office of Naval Research Contract N00014-82-C-0199
†ONR Contract N00014-82-C-0199

forms provided stationary or traveling surface waves programmable in direction, amplitude, frequency, and in the case of traveling waves, wave speed. Details of the entire active wall program are being presented elsewhere [1] and the remainder of this paper describes the electrooptical displacement sensor and subsequent measurements performed on the active wall.

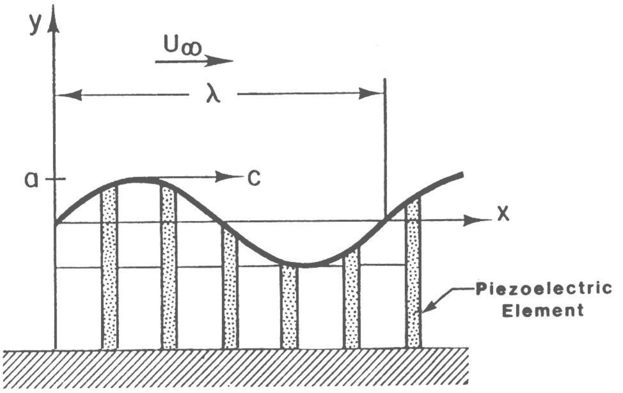

Figure 1. Illustration of Piezoelectrically Driven Active Wall.

PRINCIPLES OF OPERATION

The methodology used for the measurement technique is an adaptation of a technique developed by the author to profile roadway surfaces from a moving vehicle [2] and is illustrated in Figure 2. Two variations of the method can be implemented by choice of light source: a 1 mw Helium-Neon laser operating in the visible red at 633 nm or a high power (100 mw) light emitting diode (LED) operating in the near infrared at 933 nm. In both cases the light source is 100% amplitude modulated at a frequency of 5 kHz for use with phase sensitive detection so that a high signal-to-noise ratio and rejection of ambient light can be achieved. For the infrared version, the LED is modulated directly by the drive current, and for the visible red version, an acousto-optic modulator is used to modulate the laser. The light source is projected onto the target surface by a lens assembly oriented normal to the target surface to form a spot 1mm in diameter, a spot size small enough to resolve individual piezoelectric elements.

A portion of the light scattered from the diffusely reflecting target surface is collected by a receiving lens assembly oriented at 45° to the target surface. The lens assembly images the illuminated spot onto the center of a two element PIN photodiode detector with unity magnification. This target surface position, denoted as POSITION 1 in Figure 2, is the reference (or zero), position about which displacements are measured. At this position, the spot image is exactly centered on the two detector halves thereby causing the outputs of the two halves to be equal. By virtue of the 45° geometry, a positive or negative displacement of the target surface from the reference position causes a corresponding lateral shift of the spot image on the face of the dual detector. An example of a negative displacement is shown as POSITION 2 and is represented by the dashed lines for the target surface, light path, and spot image on the dual detector. Shifting the image of the spot on the face of the detector causes more area of the spot to fall on one half of the detector than the other, thus producing unequal outputs. The displacement signal is extracted by computing the difference and sum of the outputs of the two detector halves, then dividing the difference by the sum. The difference between the two detector halves as the image of the spot is translated from one detector half to the other, (beginning with the spot completely one half), is simply the difference in areas of a circle divided by a chord. The function is "S" shaped, with extremely good linearity for small displacements about center.

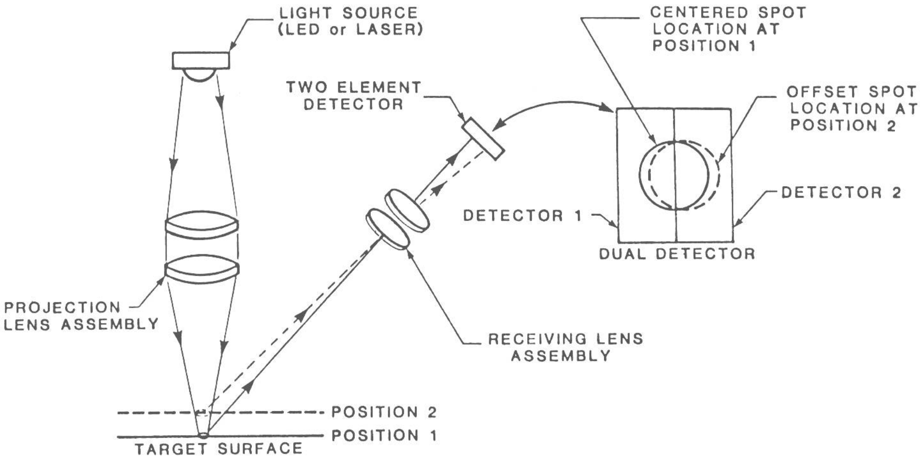

Figure 2. Optical Displacement Measuring Technique

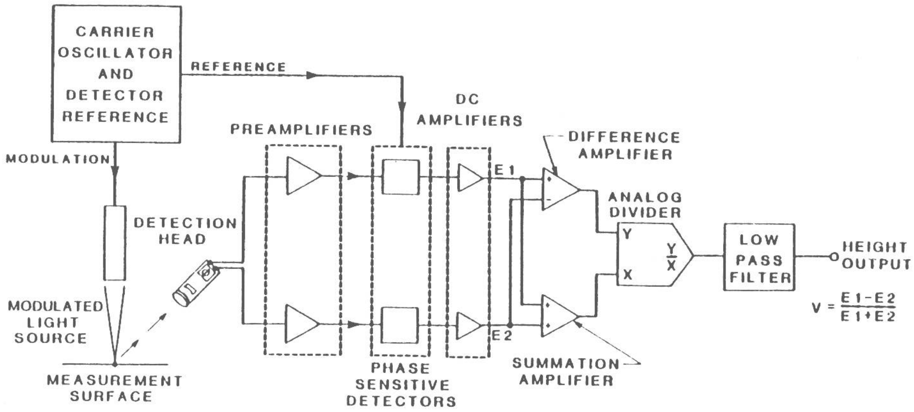

Figure 3. Electro-Optical Displacement Sensor

The sum of the two detector half outputs is a constant with respect to spot position and contains spot intensity and diameter information. The difference function is also influenced directly by spot intensity and diameter which is undesirable, as errors in the displacement measurement will occur if factors influencing spot intensity or detector sensitivity (e.g. LED or laser brightness, target surface reflectivity, water path attenuation, temperature, etc.) are variable. As the intensity and diameter data appear in both the difference and sum function, dividing the difference by the sum cancels errors associated with variable intensity or sensitivity. This method assumes uniform intensity within the spot, and no difficulties were encountered with nonuniform illumination or reflectance in this application. For details on a distance measurement system based on a similar principle but with provisions to cancel errors associated with nonuniformly reflective surfaces, the interested reader is referred to the system developed for profiling roadway surfaces [2].

A block diagram of the signal processing electronics for the displacement sensor is given in Figure 3. Design of the circuitry is straightforward and models the foregoing signal processing algorithm. A 5 kHz crystal controlled oscillator is used to drive the light modulator and to act as reference for the phase sensitive detectors. The outputs of the two detector halves are individually preamplified and filtered through active 5 kHz bandpass filters. DC restoration is accomplished through phase sensitive detectors and subsequent amplification by DC amplifiers. The DC voltages thus obtained (denoted by E1 and E2) are proportional to the light values impinging on each detector half. E1 and E2 are then processed by the differential and summation amplifiers and the resultant difference and sum are fed into the Y and X inputs of the analog divider. The quotient is (E1-E1)/(E1+E2) and is taken as the displacement signal after high frequency noise component are removed by an active low-pass filter. The signal processing circuitry was packaged in a compact (12 cm x 18 cm x 25 cm) enclosure and was completely self-contained. The light source, lens systems, and detector assembly were mounted on a precision XYZ fixture for positioning over selected areas of the active wall.

Specification for some of the component parts implemented in the laboratory system are as follows:

LED Source:	Type TIES12 (Texas Instrument) 0.91 mm (0.036-inch) diameter 50 mw @ 933 nm
LED Projection lens Assembly:	72 mm focal length 50 mm diameter
Detector:	Type PIN Spot-2D (United Detector Technology) two element discreet active surface: 2.54 x 2.67 mm (0.1 x 0.105-in.)
Detector Lens Assembly:	47 mm focal length 45 mm diameter
Laser source:	Helium-Neon Type Spectra-Physics model 138, 1.0 mw @ 633 nm
Laser Modulator:	Acoustooptic Type Anderson Labs Model PLM-5VS 40 mHz center acoustic frequency 100% square wave modulation @ 5 kHz

SENSOR CALIBRATION AND FREQUENCY RESPONSE

The electrooptic displacement sensor was calibrated with a fixture constructed specifically for the task. The calibration fixture was fabricated by using a precision micrometer and ball configuration in conjunction with a 10:1 mechanical reduction arm to provide precise control over the reference surface. Thus 0.010-inch (254 μm) of travel on the micrometer head (which was readable to 0.0001-inch or 2.54 μm) produced 0.001-inch (25.4 μm) of travel at the reference surface. Precision ball bearings were used for the fulcrum.

Figure 4 is a typical response plot of the displacement sensor taken with the calibration fixture. The fixture was immersed in a transparent water tank for this test, with the reference surface set 15 cm from the entry point of the light beam. The infrared LED was used for the light source and the spot projection was directed into the tank normal to the top wall surface. The received light was collected through the adjacent tank side wall by the receiving lens which was oriented at 45° to the tank side wall. This resulted in a water path angle of 32° by virtue of refraction at the water/air interface. Linearity and resolution over the 25 μm peak-to-peak range is extremely good, as evidenced in Figure 4. Responsivity of the displacemenmt sensor in this configuration was measured to be 61.58 μm/volt.

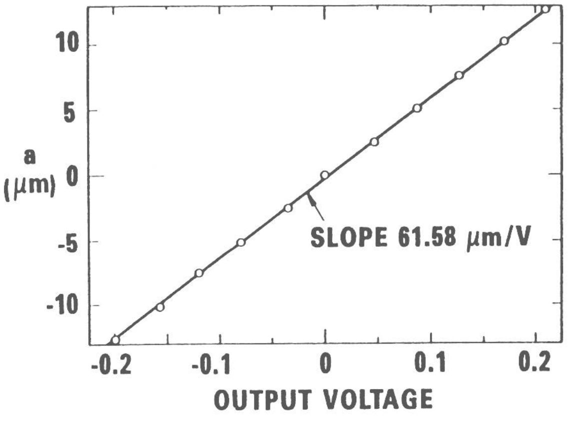

Figure 4. Displacement Calibration For Electro-Optical Sensor

Calibration data were taken in a total of four different configurations: in both air and water, and with both LED and laser light sources. The laser source has three distinct advantages and two distinct disadvantages for this application. First, the laser provides a much more intense source of light and operates at a wavelength which has little loss in water. The LED source, at 933 nm, is attenuated by the absorption band in water near 944 nm, presenting a signal strength problem for long water path distances. Second, the laser can be focused to a much smaller spot on the target surface, providing superior spatial resolution. The LED source cannot be focused efficiently to a spot much smaller than the physical diameter of the active area without incurring significant losses in intensity. Finally, the He-Ne laser operates in the visible red (as opposed to IR for the LED), making alignment of the system an easier task.

The disadvantages of using a laser are expense and stability. Most commercially available lasers in this power range, although relatively inexpensive in themselves, cannot be directly modulated. An acousto-optical modulator was used to provide the required 5 kHz subcarrier, and the cost of the modulator was more than that of the laser itself. Secondly, the laser must have a stabilized output relatively free from the noise components associated with the intermodulation products of multiple optical frequencies. These products commonly occur in the frequency range of 1 to 100 kHz, which is in-band to the 5 kHz subcarrier frequency. The noise components appear as sidebands about the 5 kHz subcarrier frequency and thus cannot be filtered easily. The analog division process removes most of the amplitude modulated noise components, but improvements in signal to noise ratios can be gained through the use of stabilized lasers.

The frequency response of the displacement monitor was measured by inserting an analog multiplier between the detector preamplifier and the remainder of the signal processing electronics. Light input to the detectors was held constant while the frequency of an external oscillator connected to the control input of the multiplier was varied. The frequency response curve is given in Figure 5 and shows reasonably flat response out to about 60 Hz with a roll off of approximately 8 dB/octave after the breakpoint. Response of the displacement sensor is

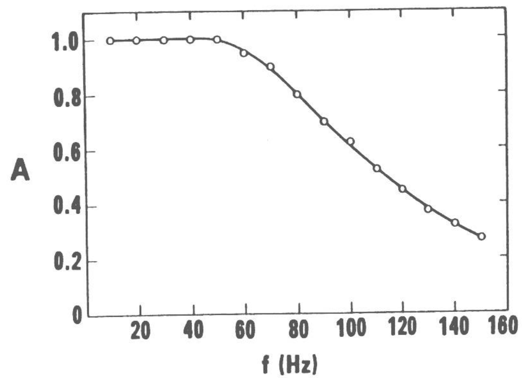

Figure 5. Amplitude Response For Electro-Optical Sensor

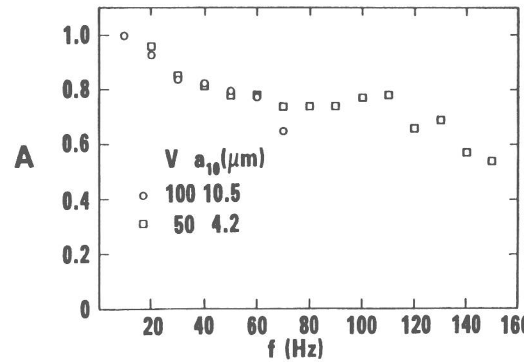

Figure 7. Wave Amplitude Response For Active Wall

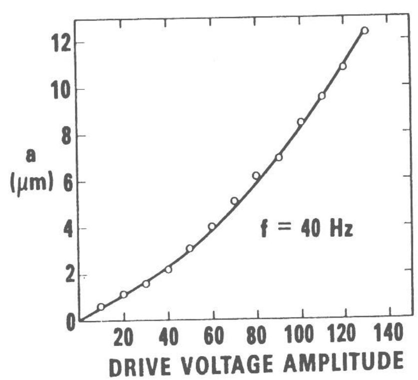

Figure 6. Wave Amplitude Calibration For Active Wall

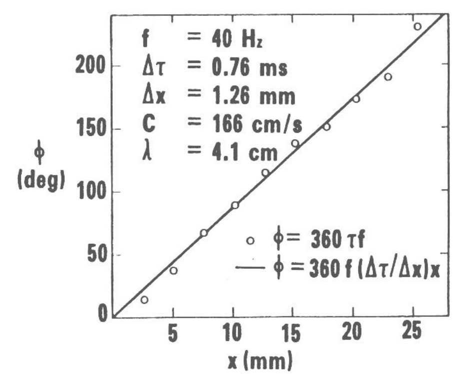

Figure 8. Phase Response For Active Wall

an adjustable parameter and is controlled by the Q of the 5 kHz bandpass amplifier, design of the output low pass filter, and (somewhat) on the selection of carrier frequency.

ACTIVE WALL MEASUREMENTS

Actual measurements made on the prototype active wall are given in Figures 6, 7 and 8. In Figure 6, the amplitude response of an individual element of the active wall is plotted as a function of applied driving voltage at a fixed frequency of 40 Hz. Figure 7 shows the frequency response of the same element plotted as a function of drive frequency for an applied voltage of 150V peak-to-peak. For both Figure 6 and 7 the raw data obtained from the displacement monitor was corrected by the amplitude and frequency response calibrations of Figures 4 and 5. Figure 8 shows the longitudinal phase response of the active wall when set up to produce a traveling wave. The data were taken by translating the displacement monitor along the length of the active wall (transversing from element to element) at a fixed standoff distance. The wall demonstrated excellent phase linearity over a distance of approximately 30 mm (1.2 in.).

CONCLUSIONS

In summary, a methodology for producing noncontacting displacement measurements through air and water path distances to surfaces possessing very small absolute displacements has been described. Actual measurements have been performed on a piezoelectrically driven active wall with successful results.

ACKNOWLEDGMENTS

The author wishes to acknowledge sponsorship of the Office of Naval Research for the reported work, the many helpful discussions on measurement technique with Mr. H. Stanley Silvus, Jr, and Dr. Joel T. Park, and construction of the project hardware by Mr. Harold F. Donoho, Jr.

REFERENCES

1. Park, J. T., Silvus, H. S., Jr., and Cerwin, S. A., "An Active Wall Device for the Generation of Small Traveling Surface Waves," Review of Scientific Instrumentation (submitted for publication).

2. King, J. D., and Cerwin, S. A., "System for Inventorying Road Surface Topography (SIRST)," U. S. Department of Transportation, Federal Highway Administration, Final Report Contract No. DOT-FH-118498, FHWA/RD-82/062, Aug. 1982.

AN OPTICAL TECHNIQUE FOR MEASURING THE FLOW-INDUCED MOTION OF A COMPLIANT SURFACE

M. Gad-el-Hak
Flow Research Company
Kent, Washington

ABSTRACT

The flow-induced motion of a compliant surface was measured using a novel remote optical technique. The "Laser Displacement Gauge" employs a Reticon camera equipped with a linear array of 256 photodiodes spaced 25 micron apart. A vertical beam of laser light produces a bright spot when it intersects the elastic or the viscoelastic compliant material, which contains minute amounts of Rhodamin-6G fluorescent dye. The axis of the photodiode array was aligned with the vertical laser beam. Thus, the digital output resulting from the continuous scanning of the array indicates the vertical displacement of the compliant surface. The system has a frequency response of 1 kHz, and resolves vertical displacements as low as 0.002 cm. The device was used to measure the characteristics of two classes of hydroelastic instability waves that form on elastic or viscoelastic compliant surfaces as a result of the interaction with a turbulent boundary layer.

1. INTRODUCTION

The motion of a fluid over a surface which complies to the flow offers the potential for a rich variety of fluid/surface interactions. Compliant surfaces are currently finding many engineering applications such as sound absorption in aero-engines, vibration reduction in Naval vessels, and noise shielding in sonar arrays. Moreover, intensive research is currently conducted to find compliant surfaces that will reduce the skin-friction drag on moving vehicles.

The design of a compliant coating to achieve a particular objective is a complex task requiring the determination of the surface response to a specific flow disturbance. This response is excited by the hydrodynamic forces and results in a surface motion which in turn acts on the flow field near the interface. Waves that form on the compliant surface can be either stable, unstable or neutral.

There exists a need for the development of reliable techniques to measure the compliant surface response under a variety of flow conditions. The device needed should be accurate, have a fast response, and not interfere with the observed phenomenon. Very few such devices exist today. Grosskreutz [1] used a Schlieren apparatus to measure the motion of a homogeneous but nonisotropic compliant surface made of rubber and subjected to a turbulent boundary layer in a water tunnel. He computed the frequency and the wavenumber dependence of the flexibility of the compliant wall using the third-octave-spectra of the surface motion. Ash et al. [2] used a similar Schlieren method to provide flash photos of a compliant surface deformation in a wind tunnel. Dinkelacker et al. [3] placed a 97 mm pressure transducer containing several hundered membranes under a turbulent boundary layer. The device served as the mirror in a Michelson interferometer. High speed photographs of the fringe patterns in the interferometer were used to compute the dimensions and the speed of convected turbulent pressure fluctuations. More recently, Rathsam et al. [4] measured the "pre-instability", microscopic surface motion on a PVC plastisol in a turbulent boundary layer. Their laser/optics system sensed the instantaneous slope and the frequency of motion on the compliant surface where a focused laser beam was reflected. This device is incapable of directly measuring the amplitude of the surface motion, however, Rathsam et al. inferred the amplitude from the measured slope spectra by assuming a dispersion relation for the compliant surface response.

The remote optical technique presented in this paper is used to measure the flow-induced motion of a compliant surface. The technique is particularly suited for studying hydroelastic instability waves that form on an elastic or a visco-elastic compliant surface as a result of the interaction with a turbulent boundary layer. The waves' amplitude, wavelength and phase speed are directly measured with this linear device.

2. EXPERIMENTAL EQUIPMENT AND PROCEDURE

2.1 The Laser Displacement Gauge

The laser displacement gauge (LDG) is a remote optical device used in the present investigation to measure the compliant surface vertical displacement. The technique was originally developed for measuring wind-waves [5,6]. Its first use for measuring compliant surface deformation was reported by Gad-el-Hak et al. [7,8]. The system employs a Reticon camera (Model LC 600V) driven by a controller (Reticon Corporation, Model RS605). An optical interface is created at the surface of the compliant material, which contained minute amounts of Rhodamin-6G fluorescent dye, by projecting a 4 Watt vertical beam of argon-ion laser (Spectra Physics, Model 164-05) having a diameter of 1 mm. The displacement of this optical interface is measured by electronically scanning the photodiode array housed in the Reticon camera.

The axis of the photodiode array is aligned with the vertical laser beam above the fluid/compliant coating interface. The optical interface is imaged onto the photodiode array via a set of lenses and extension tubes. The linear photodiode array is composed of 256 elements spaced 25 μm apart. The aperture width of the array is also 25 μm. the spatial resolution, which is the same in both the vertical and longitudinal directions, depends on the field of view. For example, the spatial resolution is 0.01 cm for a field of view of 2.5 cm. In this case, the horizontal spatial resolution is only about one-tenth of the diameter of the laser beam. The scanning rate of the array ranges from 0.4 to 40 ms. The LDG is a digital device with practically no electronic drift. The digital output from the controller is a time series of integers from 1 to 256 updated at a frequency of the scanning rate. Each integer corresponds to the n^{th} photodiode on which the optical interface is imaged during each scan. The digital output is recorded and analyzed on-line with a NOVA minicomputer system.

Calibration of the LDG is made by displacing the Reticon camera, which is fixed on an accurate traverse mechanism, to several vertical positions with predetermined increments. A second-degree polynomial is best-fitted through the calibration points to account for nonlinearity resulting from the aberration of the optical lenses. The ratio of the coefficients of the nonlinear and linear terms was typically 10^{-4}. For practical purposes, the displacements may be considered to be linearly porportional to the LDG output.

The Reticon camera is mounted so that it looks down onto the compliant surface at a nearly horizontal angle. This arrangement minimizes blockage of the optical interface by the wave crests between the laser beam and the tank wall on the side where the camera is mounted. This blockage occurs most often near the troughs of the waves, where the wave profiles are relatively smooth. Whenever a blockage occurs, the photodiode array loses its object (i.e. the optical interface) and the maximum diode number of 256 is registered by the controller. Therefore either a sharp jump or a sharp spike, depending on the duration of the blockage, appears on the measured wave profiles. To remove the sharp jumps or spikes the computer was programmed to replace them with a straight line that connects the points before and after each jump or spike.

In the present experiments the laser displacement gauge was set to have a frequency response of 1 kHz and to resolve vertical displacments as low as 0.002 cm.[1] The surface deformations were also recorded using a 16 mm movie camera moving with the plate (Section 2.2). For the elastic surface, the camera was mounted to the side to capture a side view of the instability waves; while for the viscoelastic surface a top view was more suited to observe the instabilities developing on such a surface.

2.2 Flow Facility

The Flow Research 18-m towing tank was used in the present experiments. The 1.2 m wide, 0.9 m deep water channel has been described by Gad-el-Hak et al. [9]. To generate a turbulent boundary layer, a flat plate was rigidly mounted under a carriage that rides on two tracks mounted on top of the towing tank. During towing, the carriage was supported by an oil film which insured a vibrationless tow, having an equivalent freestream turbulence of about 0.1 percent. The carriage was towed by two cables driven through a reduction gear by a 1.5 hp Boston Ratiotrol motor. The towing speed was regulated within an accuracy of 0.1 percent. The system was able to achieve towing speeds between 20 and 140 cm/sec for the present study. The flat plate used in the present experiment has an aluminum frame that provided a flat bed for the Plexiglas working surface. The gaps in the aluminum frame were filled with lightweight styrofoam and the frame was painted with marine enamel to prevent corrosion. The whole structure was buoyant in water and was flat to within 0.2 mm. Care was taken to avoid leading-edge separation and premature transition by having an elliptic leading edge and an adjustable lifting flap at the trailing edge. The flap was adjusted so that the stagnation line near the leading edge was located on the working surface. The working surface was smooth and was 210 cm long and 106 cm wide. A 45 cm by 95 cm well was built into the working surface for placing compliant materials of up to 1 cm in thickness.

Trips were used to generate a fully-developed turbulent boundary layer. The trips were brass cylinders with 0.32 cm diameter and 0.25 cm height placed 20 cm behind the leading edge, and having their axes perpendicular to the flat plate. During towing, the plate and the movie cameras moved at a speed U_∞, while the Reticon camera and the vertical laser beam were fixed in space.

2.3 Compliant Material

A nearly-ideal elastic compliant surface and an incompressible viscoelastic one were used in the present investigation. The elastic coating was made of commercially available Knox gelatins. The gelatin powder was dispersed in boiling water, followed by the addition of an equal amount of room-temperature water. The concentration of the gelatin was varied in the range of 1 to 6 parts of weight of gelatin per 100 parts of water. The mixture was poured into the well in the flat plate and allowed to gel for 16 hours before using for a maximum of 8 hours, then a new coating was formed for the next series of runs. Care was taken to insure that the compliant surface was smooth and flush with the rest of the Plexigas working surface.

---

[1] The field of view is then about 0.5 cm.